




Long-term Photometric Study of the Pre-main Sequence Star V1180 Cas

Asen Mutafov¹, Evgeni Semkov¹, Stoyanka Peneva¹, and Sunay Ibryamov² 

¹Institute of Astronomy and National Astronomical Observatory, Bulgarian Academy of Sciences, BG-1784, Sofia, Bulgaria; amutafov@astro.bas.bg

²Department of Physics and Astronomy, Faculty of Natural Sciences, University of Shumen, 115, Universitetska Str., 9700 Shumen, Bulgaria

Received 2022 September 3; revised 2022 October 10; accepted 2022 October 12; published 2022 December 7

Abstract

In this paper results from the optical photometric observations of the pre-main sequence star V1180 Cas are reported. The star is a young variable associated with the dark cloud Lynds 1340, located at a distance of 600 pc from the Sun in the star-forming region in Cassiopeia. V1180 Cas shows large amplitude variability, interpreted as a combination of accretion-induced and extinction-driven effects. Our data from *VRI* CCD photometric observations of the star were collected from September 2011 to February 2022. During our monitoring, we recorded several brightness dips with large amplitudes of up to 5 mag (*I* band). At the same time, increases in brightness over periods of several weeks have also been recorded. In this paper, we compare the photometric data obtained for V1180 Cas with observations of other low-mass pre-main sequence objects.

Key words: stars: variables: T Tauri – Herbig Ae/Be – stars: pre-main sequence – stars: evolution

1. Introduction

One of the main fundamental characteristics of young stellar objects is their photometric variability in the optical and near-infrared (near-IR) range. This variability manifests itself as temporary dips in the brightness (eclipses), transient increases in brightness (outbursts), and periodic or non-periodic brightness changes on short or long-timescales. Photometric variability with amplitudes of different magnitudes and periodicity can be observed in both types of pre-main sequence (PMS) stars—the widespread low-mass ($M \leq 2 M_{\odot}$) T Tauri stars and the more massive Herbig Ae/Be (HAEBE) stars (Herbst et al. 1994; Herbst et al. 2007). It is widely accepted (Bertout 1989; Appenzeller & Mundt 1989) that PMS stars can be divided into two subclasses based on the presence of an accretion disk—classical T Tauri (CTT) stars surrounded by a massive accretion disk and weak line T Tauri (WTT) stars without indications of disk accretion. While the variability of WTT stars is most often explained by rotational modulation of cool spots on their surface, CTT stars are characterized by variability with large amplitudes. This can be explained by magnetically channeled accretion from the circumstellar disk onto the stellar surface. This explanation is summarized in the review work of Herbst et al. (2007).

A significant part of HAEBE stars and some early type CTT stars manifest strong photometric variability with sudden quasi-Algol drops in brightness and amplitudes up to $2^m.5$ (*V*) (Natta et al. 1997; van den Ancker et al. 1998; Herbst & Shevchenko 1999). This group of PMS objects with masses similar to or greater than a solar mass are named UXors after their prototype UX Orionis. They show an increase in polarization and specific color variability (“blueing effect”) at the deep minima in

brightness. One of the most widespread explanations of their variability is a variable extinction from dust clumps or filaments passing through the line of sight to the star (Grinin et al. 1991; Dullemond et al. 2003). Normally, when the star is covered by clouds of dust located along the line of sight, it becomes redder. But when the obscuration rises sufficiently the scattered part of the light in the total observed light becomes considerable and the star color gets bluer.

Kun et al. (1994) first recognized V1180 Cas as a young variable object with a strong H_{α} emission, associated with the dark cloud Lynds 1340 in the star-forming region in Cassiopeia (Lynds 1962). Lynds 1340 is a small dark cloud with area 0.001 square degrees and opacity class 5, located at a distance of 600 pc from the Sun. The photometric observations performed by Kun et al. (2011) during the period from October 1999 to February 2011 show variability with an amplitude of about 6 mag (I_C band). Variability with such a large amplitude is consistent with that of known eruptive young stellar objects, but the observed characteristic timescales of the faint and bright phases differ from those of the eruptive PMS stars from FU Orionis (FUor) and EX Lupi (EXor) type.

Kun et al. (2011) noted that the color–magnitude diagram (I_C versus $R_C - I_C$) displays reddening while a weakening of the brightness of the star occurs. They determined the spectral type of V1180 Cas as K7-M0; the luminosity as $L/L_{\odot} \approx 0.07$ with an effective temperature $T_{\text{eff}} = 4060$ K of the K7 spectral type; the equivalent widths of H_{α} range from 300 to 900 Å and the mass accretion rate is $> 1.6 \times 10^{-7} M_{\odot} \text{ yr}^{-1}$ ($\text{Ca II } \lambda 8542$). The authors suggest that it is necessary to refine the current picture of the mechanisms of episodic accretion bursts at the time. They presume that V1180 Cas may be a new member of unclassified eruptive young stars.

Table 1
CCD Cameras and Optical Specifications

| Telescope | CCD Camera Type | Size (px) | Field (arcmin) | Pixel Size (μm) | Scale ($''/\text{px}$) | RON ($e^- \text{rms}$) | Gain (e^-/ADU) |
|------------|-----------------|--------------------|--------------------|---------------------------------|-----------------------------|-----------------------------|------------------------------|
| 2 m RCC | VersArray 1300B | 1340 \times 1300 | 5.8 \times 5.6 | 20.0 | 0.26 | 2.00 | 1.0 |
| 2 m RCC | ANDOR iKon-L | 2048 \times 2048 | 6.0 \times 6.0 | 13.5 | 0.17 | 6.90 | 1.1 |
| Schmidt | FLI PL16803 | 4096 \times 4096 | 73.8 \times 73.8 | 9.0 | 1.08 | 9.00 | 1.0 |
| 60 cm Cass | FLI PL9000 | 3056 \times 3056 | 16.8 \times 16.8 | 12.0 | 0.33 | 8.50 | 1.0 |
| 1.3 m RC | ANDOR DZ436-BV | 2048 \times 2048 | 9.6 \times 9.6 | 13.5 | 0.28 | 8.14 | 2.7 |

Near-IR monitoring of the object for the period September–August 2013 was reported by Antonucci et al. (2013). The authors recognized two major outburst events and plot the $[J-H]$ versus $[H-K]$ two-color diagram. According to them, the description of the color variation cannot be pure extinction alone, which is in agreement with the conclusions of Kun et al. (2011). Using their optical and near-IR emission observations, Antonucci et al. (2014) calculated a mass accretion rate of $3 \times 10^{-8} M_{\odot} \text{yr}^{-1}$. The first X-ray detections of V1180 Cas are reported in the paper Antonucci et al. (2015). The authors have performed simultaneous observations in X-ray, JHK photometry and J -band spectroscopy. From the observed Chandra signal the authors estimate the X-ray luminosity $L_X(0.5-7 \text{ keV})$ in the range $0.8 \div 2.2 \times 10^{30} \text{ erg s}^{-1}$. Based on the spectral energy distribution the authors inferred a stellar luminosity of $0.8-0.9 L_{\odot}$. Furthermore, the measured X-ray flux emission levels are on the order of $5 \times 10^{30} \div 1 \times 10^{31} \text{ erg s}^{-1}$. The authors concluded that the photometric behavior of V1180 Cas might be explained by a combination of accretion-induced and extinction-driven effects.

In our first paper (Mutafov et al. 2018) we reported results from VRI photometric monitoring of V1180 Cas in the period from September 2011 to April 2018. During this period we observed drops in stellar brightness with amplitude up to 3 mag (I_C). In this paper, we present data from the continuation of this multicolor optical monitoring until February 2022 and an analysis of the observed photometric variability of the star.

2. Observations

The CCD observations of V1180 Cas were performed in two observatories with four telescopes: the 2 m Ritchey-Chrétien-Coudé (RCC), the 50/70 cm Schmidt and the 60 cm Cassegrain telescopes of the Rozhen National Astronomical Observatory (Bulgaria) and the 1.3 m Ritchey-Chrétien (RC) telescope of the Skinakas Observatory of the University of Crete (Greece).³ The observations were performed with five different types of CCD cameras: ANDOR iKon-L and VersArray 1300B on the 2 m RCC telescope, ANDOR

DZ436-BV on the 1.3 m RC telescope, FLI PL16803 on the 50/70 cm Schmidt telescope, and FLI PL9000 on the 60 cm Cassegrain telescope. The technical parameters and specifications of the used CCDs are summarized in Table 1. Observational procedure and data reduction process are described in Ibraymov et al. (2015). All frames were taken through a standard Johnson-Cousins set of filters. The observations in all filters (VRI) are not simultaneous and have total duration of 20–30 minutes. During this time there is no significant change in the brightness of the star which could lead to significant changes of the color index.

In order to facilitate transformation from instrumental measurement to the standard Johnson-Cousins system, eight stars in the field of V1180 Cas were calibrated in VRI bands. Calibration was made during six clear nights in 2011, 2012 and 2015 with the 1.3 m RC telescope of the Skinakas Observatory. Standard stars from Landolt (1992) were used as reference. The finding chart of the comparison sequences is presented in Figure 1. The comparison stars are labeled from A to H in order of their V magnitudes. The field is $15' \times 15'$, centered around V1180 Cas. North is at the top and east to the left. The chart is retrieved from the STScI Second Generation Digitized Sky Survey (Red). Table 2 contains the coordinates and the photometric data for the VRI comparison sequence. Our data were analyzed using fixed apertures for V1180 Cas which were chosen to be $4''$ in radius. The background annulus was taken from $13''$ to $17''$.

3. Results and Discussion

The results of our multicolor photometric CCD observations of V1180 Cas in the period from September 2011 to February 2022 are summarized in Table 3. The columns provide the Julian date (JD) of observation, VRI magnitudes and the telescope used. In the column Telescope, the abbreviation 2 m denotes the 2 m RCC telescope, Sch—the 50/70 cm Schmidt telescope, 60 cm—the 60 cm Cassegrain telescope and 1.3 m—the 1.3 m RC telescope. The values of instrumental errors are in the range $0^{\text{m}}01-0^{\text{m}}02$ (for I and R) and $0^{\text{m}}01-0^{\text{m}}03$ (for V). The VRI -light curves of V1180 Cas during the period of our observations are plotted in Figure 2. In most cases, the size of error bars is smaller than the size of the symbols used.

³ Skinakas Observatory is a collaborative project of the University of Crete, the Foundation for Research and Technology—Hellas, and the Max-Planck-Institut für Extraterrestrische Physik.

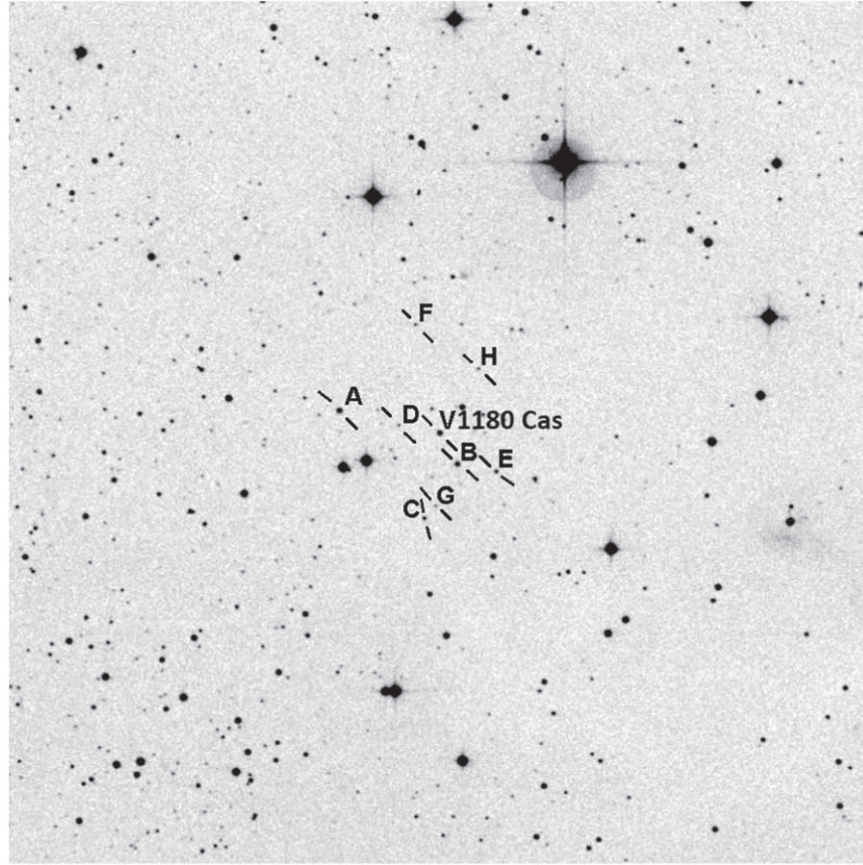


Figure 1. The finding chart of the comparison sequences.

Table 2
Coordinates and Photometric Data for the *VR*I Comparison Sequence

| Standard | $\alpha(2000)$ | $\delta(2000)$ | V | σ_V | R | σ_R | I | σ_I |
|----------|----------------|----------------|-------|------------|-------|------------|-------|------------|
| A | 02 33 25.2 | 72 43 54.9 | 16.84 | 0.04 | 15.78 | 0.03 | 14.39 | 0.03 |
| B | 02 32 58.0 | 72 42 54.5 | 17.64 | 0.03 | 16.29 | 0.04 | 14.68 | 0.03 |
| C | 02 33 06.0 | 72 41 58.8 | 18.68 | 0.05 | 17.58 | 0.03 | 16.46 | 0.04 |
| D | 02 33 11.3 | 72 43 37.2 | ... | ... | 18.79 | 0.07 | 16.54 | 0.07 |
| E | 02 32 48.7 | 72 42 45.0 | 18.69 | 0.05 | 17.60 | 0.03 | 16.56 | 0.03 |
| F | 02 33 06.7 | 72 45 20.9 | 19.63 | 0.03 | 18.59 | 0.07 | 17.51 | 0.07 |
| G | 02 33 03.2 | 72 42 11.9 | ... | ... | 19.15 | 0.07 | 17.67 | 0.06 |
| H | 02 32 52.0 | 72 44 32.9 | 19.73 | 0.05 | 18.72 | 0.06 | 17.68 | 0.05 |

During the period from 2011 to 2020, our data show very strong photometric variability with large amplitude variations ($\Delta I \sim 5$ mag). The same brightness variability was also registered in the previous studies of Kun et al. (2011), Antonucci et al. (2013, 2014) and Lorenzetti et al. (2015). Most of the time, the I band brightness of the star is kept in the range of 15–16 mag, which is considered to be the maximum light in the previous studies. However, during these periods there are changes in brightness with small amplitudes, which are characteristic of T Tauri stars.

Our photometric data over the same time period also display another type of variability, deep declines in brightness for which no periodicity is observed. We have registered four deep minima in brightness in the light curve of V1180 Cas: the first deep minimum was registered in September 2013, the second in December 2017, the third in February–March 2019 and fourth in January 2020. Therefore, the long-term light curve of V1180 Cas is similar to that of other low-mass young stars like GM Cep (Semkov & Peneva 2012; Semkov et al. 2015; Mutafov et al. 2019), 2MASS J22534654+6234582

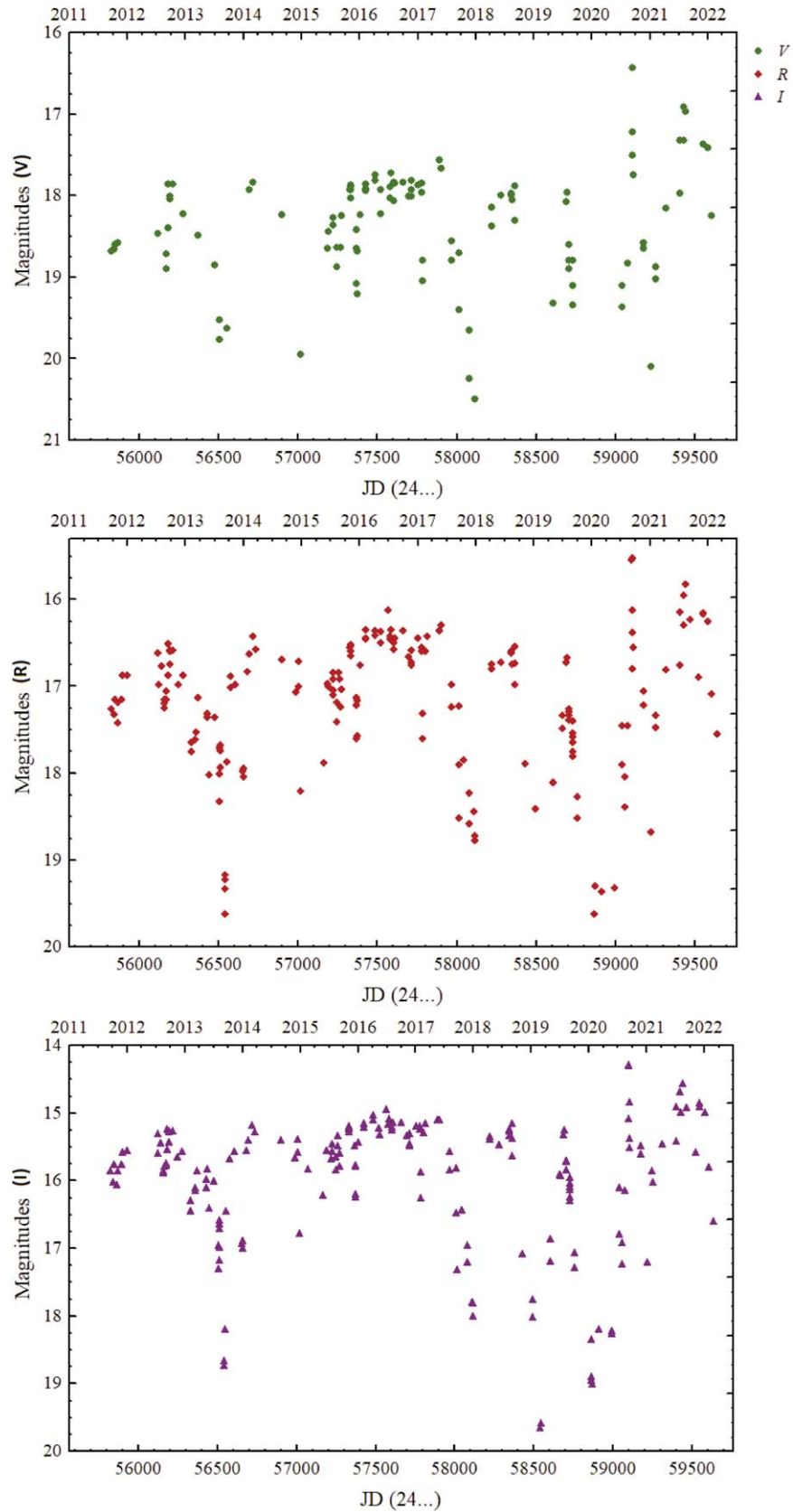


Figure 2. *VRI* light curves of V1180 Cas in the period September 2011–February 2022.

Table 3
VRI Photometric Observations of V1180 Cas

| JD (24...) | <i>V</i> | <i>R</i> | <i>I</i> | Tel | JD (24...) | <i>V</i> | <i>R</i> | <i>I</i> | Tel |
|------------|----------|----------|----------|-------|------------|----------|----------|----------|-----|
| 55824.45 | 18.68 | 17.26 | 15.86 | 1.3 m | 57603.49 | 17.84 | 16.50 | 15.21 | 2 m |
| 55842.39 | 18.66 | 17.33 | 16.02 | 1.3 m | 57605.49 | 18.07 | 16.57 | 15.25 | Sch |
| 55848.40 | 18.60 | 17.16 | 15.76 | 1.3 m | 57607.47 | 17.85 | 16.45 | 15.14 | Sch |
| 55865.40 | | 17.42 | 16.06 | 2 m | 57664.46 | 17.84 | 16.36 | 15.14 | Sch |
| 55866.50 | 18.58 | 17.19 | 15.85 | 2 m | 57698.36 | 18.01 | 16.66 | 15.33 | Sch |
| 55892.34 | | 17.15 | 15.76 | 2 m | 57714.43 | 17.81 | 16.59 | 15.31 | 2 m |
| 55896.35 | | 16.88 | 15.58 | Sch | 57715.42 | 18.01 | 16.76 | 15.45 | 2 m |
| 55925.33 | | 16.87 | 15.55 | Sch | 57716.43 | 17.93 | 16.73 | 15.48 | 2 m |
| 56122.52 | 18.46 | 16.62 | 15.30 | Sch | 57756.33 | 17.87 | 16.45 | 15.20 | Sch |
| 56123.51 | | 16.98 | 15.60 | Sch | 57781.26 | 17.96 | 16.55 | 15.20 | Sch |
| 56141.54 | | 16.77 | 15.44 | 1.3 m | 57782.33 | 17.85 | 16.60 | 15.23 | 2 m |
| 56159.50 | | 17.20 | 15.86 | Sch | 57785.28 | 19.05 | 17.61 | 16.25 | 2 m |
| 56160.50 | | 17.25 | 15.88 | Sch | 57786.31 | 18.80 | 17.32 | 15.87 | 2 m |
| 56161.52 | | 17.15 | 15.79 | Sch | 57801.26 | | 16.60 | 15.29 | Sch |
| 56173.47 | 18.72 | 17.06 | 15.74 | 1.3 m | 57817.23 | | 16.43 | 15.16 | Sch |
| 56174.48 | 18.90 | 17.15 | 15.77 | 1.3 m | 57893.54 | 17.56 | 16.36 | 15.10 | 2 m |
| 56182.41 | 18.40 | 16.87 | 15.54 | 1.3 m | 57904.54 | 17.66 | 16.30 | 15.10 | Sch |
| 56183.46 | 17.86 | 16.51 | 15.23 | 1.3 m | 57968.49 | 18.80 | 17.24 | 15.84 | Sch |
| 56193.45 | 18.01 | 16.59 | 15.28 | 1.3 m | 57969.47 | 18.56 | 16.98 | 15.57 | Sch |
| 56193.47 | 18.04 | 16.60 | 15.27 | Sch | 58011.43 | 18.70 | 17.23 | 15.82 | Sch |
| 56194.46 | | 16.75 | 15.43 | Sch | 58012.43 | 19.40 | 17.91 | 16.47 | Sch |
| 56214.33 | 17.86 | 16.59 | 15.26 | 2 m | 58013.46 | ... | 18.52 | 17.31 | Sch |
| 56249.37 | | 16.98 | 15.65 | Sch | 58043.41 | | 17.85 | 16.43 | Sch |
| 56275.37 | 18.22 | 16.87 | 15.57 | 2 m | 58080.39 | 19.65 | 18.23 | 16.95 | Sch |
| 56328.37 | | 17.76 | 16.44 | Sch | 58081.40 | 20.24 | 18.58 | 17.21 | Sch |
| 56329.29 | | 17.65 | 16.30 | Sch | 58109.42 | | 18.44 | 17.80 | Sch |
| 56356.29 | | 17.62 | 16.14 | 60 cm | 58113.34 | 20.50 | 18.72 | 17.81 | Sch |
| 56357.29 | | 17.53 | 16.10 | 60 cm | 58114.35 | | 18.77 | 18.00 | Sch |
| 56371.29 | 18.49 | 17.13 | 15.85 | 2 m | 58220.58 | 18.14 | 16.75 | 15.34 | Sch |
| 56428.52 | | 17.36 | 16.11 | 60 cm | 58220.59 | 18.37 | 16.80 | 15.39 | 2 m |
| 56430.50 | | | 15.98 | 60 cm | 58278.52 | 18.00 | 16.73 | 15.47 | Sch |
| 56432.49 | | 17.32 | 15.83 | 60 cm | 58343.47 | 18.00 | 16.60 | 15.24 | Sch |
| 56444.55 | | 18.02 | 16.41 | Sch | 58344.47 | 17.97 | 16.62 | 15.26 | Sch |
| 56478.53 | 18.85 | 17.36 | 16.00 | 2 m | 58346.49 | 18.05 | 16.75 | 15.34 | 2 m |
| 56507.52 | 19.76 | 18.32 | 17.30 | 2 m | 58363.50 | 17.88 | 16.54 | 15.16 | Sch |
| 56508.51 | 19.53 | 18.01 | 16.95 | 2 m | 58364.44 | | 16.74 | 15.38 | Sch |
| 56509.47 | | 17.71 | 16.59 | Sch | 58365.45 | 18.30 | 16.99 | 15.63 | 2 m |
| 56510.49 | | 17.74 | 16.71 | Sch | 58428.32 | | 17.90 | 17.08 | Sch |
| 56510.55 | | 17.68 | 16.64 | 60 cm | 58492.26 | | 18.41 | 17.75 | Sch |
| 56511.51 | | | 16.99 | Sch | 58496.28 | | | 18.01 | Sch |
| 56512.49 | | 17.94 | 17.18 | Sch | 58543.38 | | | 19.65 | Sch |
| 56540.46 | | 19.17 | 18.66 | Sch | 58544.24 | | | 19.58 | 2m |
| 56541.49 | | 19.23 | 18.73 | Sch | 58604.56 | | | 17.20 | Sch |
| 56543.48 | 20.82 | 19.62 | | 2 m | 58606.56 | 19.32 | 18.11 | 16.86 | 2 m |
| 56544.45 | 20.81 | 19.33 | 18.20 | 2 m | 58666.52 | | 17.34 | 15.92 | Sch |
| 56553.45 | 19.63 | 17.87 | 16.44 | 1.3 m | 58667.55 | | 17.48 | 15.92 | Sch |
| 56577.54 | | 16.89 | 15.67 | 60 cm | 58690.52 | 18.08 | 16.73 | 15.32 | 2 m |
| 56578.55 | | 17.02 | 15.68 | 60 cm | 58691.56 | 17.96 | 16.68 | 15.25 | 2 m |
| 56604.48 | | 16.98 | 15.57 | 60 cm | 58704.50 | 18.90 | 17.39 | 15.84 | Sch |
| 56655.32 | | 17.98 | 16.93 | Sch | 58705.49 | 18.60 | 17.27 | 15.72 | Sch |
| 56656.47 | | 17.95 | 16.88 | Sch | 58706.50 | 18.80 | 17.34 | 15.70 | Sch |
| 56657.27 | | 18.05 | 17.00 | Sch | 58707.52 | 18.80 | 17.29 | 15.71 | Sch |
| 56681.32 | | 16.83 | 15.55 | Sch | 58726.48 | 18.80 | 17.40 | 15.95 | 2 m |
| 56694.26 | 17.93 | 16.63 | 15.40 | 2 m | 58727.51 | | 17.54 | 16.03 | 2 m |
| 56715.40 | 17.83 | 16.42 | 15.18 | Sch | 58728.59 | | 17.82 | 16.30 | 2 m |
| 56738.36 | | 16.57 | 15.28 | Sch | 58729.48 | 19.34 | 17.76 | 16.23 | 2 m |
| 56899.46 | 18.24 | 16.69 | 15.40 | 1.3 m | 58730.51 | 19.10 | 17.58 | 16.09 | 2 m |
| 56988.29 | | 17.07 | 15.66 | Sch | 58730.57 | | 17.65 | 16.13 | Sch |
| 57005.34 | | 17.00 | 15.58 | Sch | 58758.26 | | 18.52 | 17.29 | Sch |

Table 3
(Continued)

| JD (24...) | V | R | I | Tel | JD (24...) | V | R | I | Tel |
|------------|-------|-------|-------|-------|------------|-------|-------|-------|-----|
| 57006.43 | | 16.71 | 15.39 | Sch | 58759.41 | | 18.27 | 17.06 | Sch |
| 57016.39 | 19.95 | 18.21 | 16.78 | 2 m | 58864.32 | | | 18.95 | Sch |
| 57074.23 | | | 15.83 | Sch | 58865.33 | | | 18.35 | Sch |
| 57164.55 | | 17.88 | 16.21 | Sch | 58867.29 | 20.75 | 19.62 | 18.90 | 2 m |
| 57187.55 | 18.65 | 16.97 | 15.55 | 2 m | 58870.32 | | 19.30 | 19.00 | Sch |
| 57190.54 | 18.44 | 17.01 | 15.55 | 2 m | 58909.25 | | 19.37 | 18.20 | Sch |
| 57220.52 | | 17.05 | 15.67 | Sch | 58993.55 | | | 18.22 | Sch |
| 57221.54 | | 17.10 | 15.67 | Sch | 58993.53 | | 19.32 | 18.27 | 2 m |
| 57223.54 | 18.36 | 16.92 | 15.56 | 2 m | 59041.51 | 19.10 | 17.46 | 16.11 | Sch |
| 57224.53 | 18.27 | 16.84 | 15.45 | 2 m | 59042.50 | 19.37 | 17.91 | 16.79 | Sch |
| 57246.53 | 18.88 | 17.41 | 15.84 | 1.3 m | 59059.44 | | 18.39 | 17.24 | Sch |
| 57247.48 | 18.64 | 17.19 | 15.65 | 1.3 m | 59060.51 | | 18.05 | 16.92 | Sch |
| 57259.45 | | 16.84 | 15.33 | Sch | 59075.34 | 18.83 | 17.46 | 16.14 | 2 m |
| 57260.47 | | 16.92 | 15.48 | Sch | 59101.50 | | 15.55 | 14.29 | Sch |
| 57271.49 | 18.64 | 17.24 | 15.79 | 2 m | 59102.40 | 16.43 | 15.52 | 14.30 | 2 m |
| 57272.47 | 18.25 | 17.04 | 15.59 | 2 m | 59103.43 | 17.50 | 16.38 | 15.08 | 2 m |
| 57330.34 | 17.93 | 16.55 | 15.24 | Sch | 59104.45 | | 16.80 | 15.51 | Sch |
| 57331.36 | 17.89 | 16.60 | 15.23 | Sch | 59105.47 | 17.22 | 16.13 | 14.83 | Sch |
| 57332.35 | 18.03 | 16.65 | 15.28 | Sch | 59109.44 | 17.75 | 16.55 | 15.37 | Sch |
| 57333.33 | 17.93 | 16.52 | 15.22 | Sch | 59176.34 | 18.65 | 17.22 | 15.60 | Sch |
| 57334.32 | 17.87 | 16.53 | 15.20 | Sch | 59177.36 | 18.58 | 17.06 | 15.48 | Sch |
| 57369.31 | 18.42 | 17.13 | 15.49 | 2 m | 59220.31 | 20.10 | 18.68 | 17.21 | 2 m |
| 57370.37 | 19.08 | 17.60 | 16.24 | 2 m | 59250.32 | 18.88 | 17.34 | 15.86 | 2 m |
| 57371.34 | 18.65 | 17.22 | 15.79 | 2 m | 59251.27 | 19.02 | 17.48 | 16.02 | 2 m |
| 57372.33 | 19.20 | 17.57 | 16.20 | Sch | 59314.58 | 18.16 | 16.81 | 15.45 | 2 m |
| 57374.34 | 18.68 | 17.17 | 15.77 | Sch | 59402.53 | 17.97 | 16.76 | 15.41 | 2 m |
| 57390.23 | 18.24 | 16.76 | 15.43 | Sch | 59403.51 | 17.33 | 16.15 | 14.90 | Sch |
| 57425.39 | 17.92 | 16.45 | 15.21 | Sch | 59426.50 | 16.91 | 15.95 | 14.69 | 2m |
| 57426.40 | 17.94 | 16.46 | 15.21 | Sch | 59428.52 | 17.32 | 16.30 | 14.99 | 2 m |
| 57427.37 | 17.86 | 16.35 | 15.16 | Sch | 59441.50 | 16.97 | 15.83 | 14.57 | Sch |
| 57483.60 | 17.75 | 16.36 | 15.03 | 2 m | 59468.45 | | 16.23 | 14.93 | Sch |
| 57484.60 | 17.81 | 16.41 | 15.10 | 2 m | 59523.33 | | 16.90 | 15.58 | Sch |
| 57522.54 | 17.93 | 16.37 | 15.22 | Sch | 59549.37 | 17.37 | 16.15 | 14.91 | Sch |
| 57523.54 | 18.22 | 16.50 | 15.32 | Sch | 59550.34 | 17.36 | 16.16 | 14.86 | Sch |
| 57565.53 | | 16.12 | 14.95 | Sch | 59582.32 | 17.42 | 16.26 | 14.99 | Sch |
| 57581.52 | 18.03 | 16.42 | 15.17 | Sch | 59605.30 | 18.24 | 17.10 | 15.80 | 2 m |
| 57582.55 | 17.89 | 16.46 | 15.16 | Sch | 59636.25 | | 17.55 | 16.60 | Sch |
| 57583.53 | 17.72 | 16.35 | 15.09 | Sch | | | | | |

(Ibryamov et al. 2020) and FHO 27 (Findeisen et al. 2013; Ibryamov & Semkov 2020). All of these objects display typical UXor variability, but are T Tauri stars from late spectral types.

The color–magnitude diagrams of V1180 Cas V versus $(V-R)$, V versus $(V-I)$ and R versus $(R-I)$ are depicted in Figure 3. The collected multicolor photometric data exhibit the typical UXor color reversal during the minima in brightness. This is a manifestation of the so-called “blueing” effect, in which the color of the star gets bluer at the minima of its brightness, in accordance with the model of dust-clump obscuration. The figure affirms that, for each of the color diagrams, a point of color reversal is observed at different star brightnesses: in the V to $(V-R)$ diagram, the point of reversal is observed at V about 19.0 mag, in the V to $(V-I)$ diagram at V about 19.2 mag and in the R to $(R-I)$ diagram at R about 17.5 mag. In the

color–magnitude diagrams of V1180 Cas, like in the case of GM Cep and V1184 Tau, the “blueing” effect is observed, as well as in $V-R$ color and in $R-I$ color (Semkov et al. 2013; Semkov et al. 2015; Mutafov et al. 2019, 2022).

Since the fall of 2020, there has been a significant change in the photometric behavior of V1180 Cas. We registered two increases in brightness (local maxima of brightness): the first one in September 2020 and the second in July/August 2021. In this case, the increase in brightness seems to be caused by increased accretion. Evidence of this is the decrease in the color indices ($V-R$ and $V-I$) of the star (Figure 3), during the increase in brightness.

PMS stars are characterized by different types of variability. In many cases, two or more different types of variability can be observed for the same star. We know objects that show both an

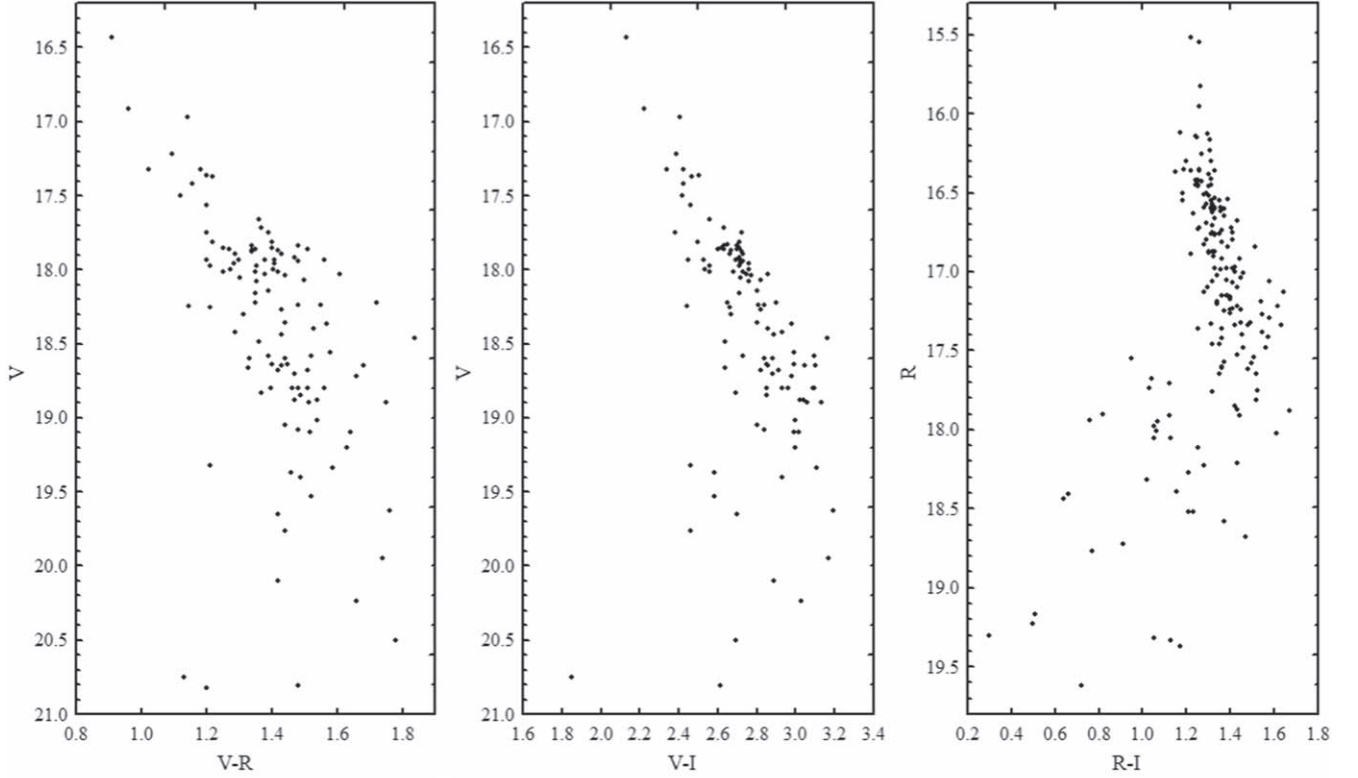


Figure 3. The color–magnitude diagrams of V1180 Cas in the period of observations September 2011–February 2022.

increase in brightness due to increased accretion and a decrease in brightness caused by variable extinction such as V582 Aur (Semkov et al. 2013; Ábrahám et al. 2018). The assumption that the observed variations in the brightness of V1180 Cas are a combination of variable accretion and variable extinction in the line of sight was made by Kun et al. (2011) and Antonucci et al. (2015). But using data from multicolor photometry, we can distinguish the two phenomena over different periods of time.

The UXor phenomenon has been discovered and defined in young stars with high and medium masses (HAEBE stars and early type CTT stars). But recently, a large number of small-mass objects have been discovered that also exhibit this type of variability (Semkov et al. 2013; Ibryamov et al. 2015; Semkov et al. 2015; Mutafov et al. 2022). This phenomenon is especially common among stars from young stellar clusters and stellar associations (Findeisen et al. 2013; Barsunova et al. 2015). This demonstrates that the processes of formation of stars with different masses proceed similarly. A significant part of the protostellar gas–dust cloud remains in the vicinity of the newly formed stars and causes variable extinction.

4. Conclusions

The last collected multicolored photometric data confirm that outside the deep minima V1180 Cas shows significant

variations of brightness lasting days and months. The same data, again, confirm that the variability of the star is dominated by the variable extinction. The *VRI* light curves of V1180 Cas are similar to other objects—GM Cep (Semkov & Peneva 2012; Semkov et al. 2015; Mutafov et al. 2022), V1184 Tau (Mutafov et al. 2019), 2MASS J22534654+6234582 (Ibryamov et al. 2020) and FHO 27 (Findeisen et al. 2013; Ibryamov & Semkov 2020). The “blueing effect” is observed during the minima of brightness which is typical for UXor variables. Color-magnitude diagrams of V1180 Cas, like the ones of GM Cep and V1184 Tau, clearly exhibit the “blueing” effect both in *V-R* and *R-I* colors (Mutafov et al. 2019, 2022). In our previous paper (Mutafov et al. 2018), we concluded that the photometric properties of V1180 Cas can be explained by a superposition of highly variable accretion from the circumstellar disk onto the stellar surface and occultation from circumstellar clumps of dust, planetesimals or from other features on the circumstellar disk. The new observational data confirm this conclusion but, additionally, we observed significant change in the behavior of the variability of the star—in the increase of its brightness, probably caused by increased accretion. An attempt at finding a periodicity of light curves was made but without a satisfactory result. The detailed explanation of this effect requires further observations.

Acknowledgments

The authors thank the Director of Skinakas Observatory Prof. I. Papamastorakis and Prof. I. Papadakis for the award of telescope time. We thank Dr. Valentin D. Ivanov (ESO) for discussions on the ideas for planetesimals. This work was partly supported by the National RI Roadmap Project (contracts D01-383/18.12.2020 and D01-176/29.07.2022) of the Ministry of Education and Science of the Republic of Bulgaria. This research has made use of NASA's Astrophysics Data System Abstract Service, the SIMBAD database and the VizieR catalog access tool, operated at CDS, Strasbourg, France.

ORCID iDs

Sunay Ibryamov  <https://orcid.org/0000-0002-4618-1201>

References

- Ábrahám, P., Kóspál, Á., Kun, M., et al. 2018, *ApJ*, **853**, 28
- Antonucci, S., Arkharov, A. A., Di Paola, A., et al. 2014, *A&A*, **565**, L7
- Antonucci, S., Arkharov, A. A., Efimova, N., et al. 2013, *ATel*, **5421**, 1
- Antonucci, S., Nucita, A. A., Giannini, T., et al. 2015, *A&A*, **584**, A21
- Appenzeller, I., & Mundt, R. 1989, *A&ARv*, **1**, 291
- Barsunova, O. Y., Grinin, V. P., Sergeev, S. G., Semenov, A. O., & Shuganov, S. Y. 2015, *Ap*, **58**, 193B
- Bertout, C. 1989, *ARA&A*, **27**, 351
- Dullemond, C. P., van den Ancker, M. E., Acke, B., & van Boekel, R. 2003, *ApJ*, **594**, L47
- Findeisen, K., Hillenbrand, L., Ofek, E., et al. 2013, *ApJ*, **768**, 93
- Grinin, V. P., Kiselev, N. N., Minikulov, N. K., Chernova, G. P., & Voshchinnikov, N. V. 1991, *Ap&SS*, **186**, 283
- Herbst, W., Eisloffel, J., Mundt, R., & Scholz, A. 2007, in *Protostars and Planets V*, ed. B. Reipurth, D. Jewitt, & K. Keil (Tucson, AZ: Univ. Arizona Press), 297
- Herbst, W., Herbst, D. K., Grossman, E. J., & Weinstein, D. 1994, *AJ*, **108**, 1906
- Herbst, W., & Shevchenko, V. S. 1999, *AJ*, **118**, 1043
- Ibryamov, S., & Semkov, E. 2020, *BulgAJ*, **32**, 96
- Ibryamov, S., Semkov, E., Peneva, S., & Gocheva, K. 2020, *RAA*, **20**, 194
- Ibryamov, S. I., Semkov, E. H., & Peneva, S. P. 2015, *PASA*, **32**, e021
- Kun, M., Obayashi, A., Sato, F., et al. 1994, *A&A*, **292**, 249
- Kun, M., Szegedi-Elek, E., Moór, A., et al. 2011, *ApJ*, **733**, L8
- Landolt, A. U. 1992, *AJ*, **104**, 340
- Lorenzetti, D., Antonucci, S., Giannini, T., et al. 2015, *ApJ*, **802**, 24
- Lynds, B. T. 1962, *ApJS*, **7**, 1
- Mutafov, A. S., Semkov, E. H., Ibryamov, S. I., & Peneva, S. P. 2019, *AIP Conf. Proc.*, **2075**, 090004
- Mutafov, A. S., Semkov, E. H., Ibryamov, S. I., & Peneva, S. P. 2022, *BAJ*, **32**, 3
- Mutafov, A. S., Semkov, E. H., Peneva, S. P., & Ibryamov, S. I. 2018, Photometric study of UX Ori type stars GM Cep and V1180 Cas, in *Proc. 11th Bulgarian-Serbian Astronomical Conf.*, 229
- Natta, A., Grinin, V. P., Mannings, V., & Ungerechts, H. 1997, *ApJ*, **491**, 885
- Semkov, E., & Peneva, S. 2012, *Ap&SS*, **338**, 95
- Semkov, E. H., Ibryamov, S. I., Peneva, S. P., et al. 2015, *PASA*, **32**, e011
- Semkov, E. H., Peneva, S. P., Munari, U., et al. 2013, *A&A*, **556**, A60
- van den Ancker, M. E., de Winter, D., & Tjin A Dje, H. R. E. 1998, *A&A*, **330**, 145